Harderian Gland Tumorigenesis: Low-Dose and LET Response

Author(s): Polly Y. Chang , Francis A. Cucinotta , Kathleen A. Bjornstad , James Bakke , Chris J. Rosen , Nicholas Du , David G. Fairchild , Eliedonna Cacao , and Eleanor A. Blakely
Source: Radiation Research, 185(5):449-460.
Published By: Radiation Research Society
DOI: http://dx.doi.org/10.1667/RR14335.1
URL: http://www.bioone.org/doi/full/10.1667/RR14335.1

RADIATION RESEARCH **185**, 449–460 (2016)
0033-7587/16 $15.00

DOI: 10.1667/RR14335.1

Harderian Gland Tumorigenesis: Low-Dose and LET Response

Polly Y. Chang,[a,b] Francis A. Cucinotta,[c] Kathleen A. Bjornstad,[b] James Bakke,[a] Chris J. Rosen,[a] Nicholas Du,[b] David G. Fairchild,[b] Eliedonna Cacao[c] and Eleanor A. Blakely[b,1]

[a] *Biosciences Division, SRI International, Menlo Park, California 94025;* [b] *Life Sciences Division, Lawrence Berkeley National Laboratory, Berkeley, California 94720; and* [c] *Department of Health Physics and Diagnostic Sciences, University of Nevada, Las Vegas, Nevada 89154*

Chang, P. Y., Cucinotta, F. A., Bjornstad, K. A., Bakke, J., Rosen, C. J., Du, N., Fairchild, D. G., Cacao, E. and Blakely, E. A. Harderian Gland Tumorigenesis: Low-Dose and LET Response. *Radiat. Res.* 185, 449–460 (2016).

Increased cancer risk remains a primary concern for travel into deep space and may preclude manned missions to Mars due to large uncertainties that currently exist in estimating cancer risk from the spectrum of radiations found in space with the very limited available human epidemiological radiation-induced cancer data. Existing data on human risk of cancer from X-ray and gamma-ray exposure must be scaled to the many types and fluences of radiations found in space using radiation quality factors and dose-rate modification factors, and assuming linearity of response since the shapes of the dose responses at low doses below 100 mSv are unknown. The goal of this work was to reduce uncertainties in the relative biological effect (RBE) and linear energy transfer (LET) relationship for space-relevant doses of charged-particle radiation-induced carcinogenesis. The historical data from the studies of Fry *et al.* and Alpen *et al.* for Harderian gland (HG) tumors in the female CB6F1 strain of mouse represent the most complete set of experimental observations, including dose dependence, available on a specific radiation-induced tumor in an experimental animal using heavy ion beams that are found in the cosmic radiation spectrum. However, these data lack complete information on low-dose responses below 0.1 Gy, and for chronic low-dose-rate exposures, and there are gaps in the LET region between 25 and 190 keV/μm. In this study, we used the historical HG tumorigenesis data as reference, and obtained HG tumor data for 260 MeV/u silicon (LET ~70 keV/μm) and 1,000 MeV/u titanium (LET ~100 keV/μm) to fill existing gaps of data in this LET range to improve our understanding of the dose-response curve at low doses, to test for deviations from linearity and to provide RBE estimates. Animals were also exposed to five daily fractions of 0.026 or 0.052 Gy of 1,000 MeV/u titanium ions to simulate chronic exposure, and HG tumorigenesis from this fractionated study were compared to the results from single 0.13 or 0.26 Gy acute titanium exposures. Theoretical modeling of the data show that a nontargeted effect model provides a better fit than the targeted effect model, providing important information at space-relevant doses of heavy ions.

INTRODUCTION

One of the primary risks associated with radiation exposure during space flight is radiation-induced cancer. The sparse data that exist on human carcinogenesis from neutrons and charged particles come from the very few studies reporting secondary cancers in radiotherapy patients treated with some of these radiations (primarily protons or neutrons). The inherent limitations of epidemiology, however, make it difficult to directly quantify health risk from most radiotherapy and other medical exposures (*1*). Epidemiological evaluation of cosmic radiation exposure and mortality or cancer risk among European airline flight crews have also not reported a clear cause-and-effect relationship between risk of any site-specific cancer and occupational exposure as a pilot or flight attendant (*2–4*).

For high-linear energy transfer (LET) radiation, the current situation is limited to extrapolating high-LET cancer risks to humans from nonhuman experimental systems. The merits of such extrapolations have recently been reviewed in NCRP Report no. 150 (*5*) where it was concluded that the significant animal database that exists for all causes of mortality from neutrons can be reasonably used to predict response in humans where no analytically useful data currently exist. These neutron results may also provide predictions of similar risks from heavy-ion exposures in space flight. However, the very limited animal studies of adverse health effects from heavy-ion exposures warrant more research to identify possible differences between neutron and HZE exposures.

The Harderian gland (HG) is an orbital gland found in the majority of land vertebrates (*6*) and is a pure ''pocket'' of epithelial and secretory cells that is naturally occurring in the mouse to lubricate the eye. There are no experimental perturbations to the native tissue environment in the F1 hybrid mouse, which serves as an ideal nontransgenic rodent model to study the impact of tissue environment to

[1] Address for correspondence: Biosciences Area, Biological Systems and Engineering Division, Lawrence Berkeley National Laboratory, Berkeley, CA 94720; email: EABlakely@lbl.gov.

tumor induction. The prevalence of naturally occurring tumors in the HG is highly dependent on the genotype of the species and strain (*7–10*). However, the historical data published by Fry *et al.* (*11–13*) and Alpen *et al.* (*14, 15*) on rodent HG tumorigenesis in the female $B6CF_1$/Anl (C57Bl/6J X BALB/CJ/ANL) mice are the single most comprehensive data set of experimental observations and dose dependence available on a specific radiation-induced tumor in an experimental animal using beams of heavy ions identical to those found in the cosmic radiation spectrum. The shape of the dose response and relative biological effects (RBEs) derived from the HG tumor experiments for heavy ions were similar to those found with fission neutrons (*16*); in any case, the high RBEs found for some of the ions, notably iron, have strongly influenced debates about astronaut risk.

Fry (*11*) found the murine HG tumorigenesis model to be a useful and appropriate experimental model for estimation of the radiation quality dependence of human cancer risk in space. It is important, for the final choice of appropriate quality factors in space, to obtain new experimental data to delineate the dose-response shape at low doses ($<$0.1 Gy) and the RBE/LET relationship while completing the radiation quality, dose and dose-rate deficiencies in existing experiments (*13, 14*). Assuming these factors are representative of, and can be extrapolated to human cancer risk, will be significant to adjusting the radiation-risk estimates that are based on epidemiological results obtained from the Radiation Effects Research Foundation [RERF; the cooperative scientific organization of Japan and the U.S. dedicated to studying health effects of atomic bomb radiation for peaceful purposes (http://www.rerf.jp/index_e.html)].

The RBE of high-LET radiation, such as iron particles, appeared to be similar to that for fission neutrons (*13, 17*). Unfortunately, there are only limited data from studies of nonhuman experimental systems at low fluences from which to estimate the late effects of chronic exposures of high-LET radiations with confidence (*16, 18, 19*). Rodent tumorigenesis data from studies with protons or iron ions each alone, or protons and iron ions sequentially combined, suggest that mean LETs of the primary cosmic rays may be insufficient to accurately evaluate the relative risks of each type of particle radiation in a field of mixed radiation qualities (*20*).

The main goal of this work is focused on investigating the effects of a broader range of particle radiation qualities and doses not previously reported on the development of HG tumors in female CB6F1 mice 16 months after exposure. The beams used in this study included 260 MeV/u silicon and 1,000 MeV/u titanium ions. A ^{137}Cesium (Cs) gamma-radiation study and 600 MeV/u iron ion study were also completed at different low-dose levels to allow comparisons with prior published work, and the calculation of RBE. Here we also report on the effects of chronic (five successive low-dose daily fractions), whole-body exposures of 1,000 MeV/u titanium ions on the development of HG tumors. The data from our work have been smoothly integrated with the prior published HG dataset in theoretical modeling of the combined data using targeted theories based on linear dose responses at low dose, as well as nontargeted assumptions based on a nonlinear threshold type response in addition to the linear dose term at low doses. Comprehensive RBE estimates are presented for different modeling approaches, and there is an emphasis on providing an alternative to the maximum RBE (RBE_{max}), which is less sensitive to low dose, low-LET data.

MATERIALS AND METHODS

Animal Procedures

The technical procedures used in the project were modeled after the original studies performed by Alpen *et al.* (*14*). Female BALB/cAnNHsd inbred mice were crossed with male C57BL/6NHsd mice to create the CB6F1/Hsd mouse model at Harlan® Laboratories Inc. (Indianapolis, IN). Source animal cohorts were maintained in the same barrier facility at the vendor for consistency. For each study, appropriate numbers of female animals (100–120 days old) were shipped directly from the vendor and held at the animal facility (BLAF) at Brookhaven National Laboratory (Upton, New York) approximately 1 week prior to the assigned beam time.

Animals were microchipped with AVID® chips for identification, weighed and randomized by weight immediately prior to whole-body particle radiation exposure. Shortly after irradiation, the mice were shipped to the animal facility at Lawrence Berkeley National Laboratory (LBNL) and maintained for 16 months. The 16-month period for tumor development is consistent with previously published methods (*13, 14*) and is the optimal time (in this F1 hybrid) when the probability of occurrence of HG tumors is considered to be near maximum, while deaths from disease and from other tumors are not significant enough to alter the statistical evaluation of the tumor prevalence data. Animals were housed 3–4 per microisolator cage and given commercial food (Purina® 5053) and water *ad libitum*. The animal room was on a 12:12 h light-dark schedule and the facility's temperature was kept at 20–22°C and relative humidity at 30–70%.

Animals were monitored at least once a day for any physical or behavioral changes that might indicate distress, discomfort, pain or injury. Mice were weighed at least once a month. If a downward trend in weight was noted, they were weighed more frequently, e.g. twice a month or even once a week. The condition was also reported to the animal core facility manager with potential follow-up by the attending veterinarian.

All procedures were compliant with the standards of the Guide for the Care and Use of Laboratory Animals of the National Institutes of Health and approved by the Animal Care and Use Committees at Lawrence Berkeley National Laboratory (LBNL; Berkeley, CA), BNL and SRI International (Menlo Park, CA).

Irradiation Procedures

Animals were exposed to charged particle beams from the NASA Space Radiation Laboratory (NSRL) at BNL (*21*). Dosimetric studies, including both depth-dose and dose-uniformity measurements, were conducted by the beamline physicists. The mice were held briefly unanesthetized in plastic boxes (40 $\times$ 40 $\times$ 73 mm) drilled with numerous holes to provide abundant airflow. Twelve boxes were assembled in an array one box deep in the 20 $\times$ 20 cm beam spot with $\pm$2.5% dose uniformity. Animals were irradiated with a single low heavy-ion dose ($\leq$0.5 Gy) of 260 MeV/u silicon (LET $\sim$ 70 keV/μm), 1,000 MeV/u titanium (LET $\sim$ 100 keV/μm) or 600 MeV/u iron ions (LET $\sim$193 keV/μm). ^{137}Cs gamma ray was used as low-LET reference. The dose rate used for each of the beams ranged between 0.2 and 0.5 Gy/min, approximating the dose rates used previously by Alpen. Cohorts

TABLE 1
Beam Energies and LET_∞

Ion	Energy (MeV/u)	Entrance LET_∞ (keV/μm)
Silicon	260	70
Titanium	1,000	100
Iron	600	193

of animals were also exposed to five fractions of 0.026 or 0.052 Gy of 1,000 MeV/u titanium ions, delivered on five successive days, to simulate chronic exposure. The frequencies of HG tumorigenesis from the fractionated study were compared to the results from single 0.13 or 0.26 Gy acute titanium exposures. Characteristics of the heavy ion beams used in this article are shown in Table 1.

During irradiation, animals on the beamline were remotely monitored in the staging area using a video camera system mounted in the irradiation cave. Control animals were included in each experimental run, the sham-treated animals were loaded into the clear plastic holders for equivalent exposure times, but were not irradiated. Since the radiation doses were small, exposure times were <1 min each. After irradiation, animals were unloaded to their housing cage with their previous cage mates and transported back to BLAF for temporary housing until shipment to the LBNL Animal Facility.

Tissue Collection and Sample Processing

Gross observations of all tissues were conducted during necropsy and recorded (this data is still in preparation and will be published elsewhere). HGs from all surviving animals were collected and animals with visibly large HG tumors were noted. Half of the collected HG tissue was fixed and the rest of the tissue was snap frozen in liquid nitrogen for further analysis. Fixed HGs were blocked, step-sectioned every 50–75 μm apart at 5 μm thickness to exhaustion and hematoxylin and eosin (H&E) stained. The slides were examined by a board-certified veterinarian histopathologist, scored, characterized and the results were recorded in an electronic data capture system. In Alpen's studies, the whole HG tissue was embedded in paraffin and multiple sections were examined microscopically. We believe that our method of thoroughly examining sections generated from exhaustive slicing of half of each HG gland is comparable to the historical work.

Data Analysis

Harderian gland tumor prevalence is expressed as the number of animals with tumor(s) divided by the total number of animals in the experimental group. There are two HG per mouse, one near each eye, and the number of tumors in each gland can be measured since multiple sections are evaluated. To be consistent with the accounting methods used by Alpen *et al*., the tally of the ''number of animals with HG tumors'' was used as the numerator for the prevalence calculation. That is, we counted the number of tumor-bearing animals and not the number of HG tumors found in the animals. Only animals that survived the 16-month period were included in the denominator when calculating prevalence.

Statistics and Modeling

Power calculations were conducted prior to the studies to determine the number of animals needed for each experiment, to obtain results that are statistically meaningful at the space-relevant low-particle radiation doses specified. Tests of statistical significance from these experiments were done for both control prevalence and tumor dose response using the two-sample test of proportions, and one-way repeated measures of analysis of variance (ANOVA), respectively.

Based on the prior work of Cucinotta and Chappell (*22*), we considered two models, one representing targeted effects (TE), which assumes a linear dose response at low doses, and one representing nontargeted effects (NTE), which assumes a nonlinear threshold type response in addition to the linear dose term at low doses, to make a fit to HG tumor response data for the current experiment. After testing for possible differences, a global fit to the current data and the prior data of Alpen *et al*. (*14*) was made. In addition, several NTE models were tested including one where the NTE term has a dependence on LET, denoted as the NTE1 model, and one where there was no LET dependence for NTE at high LET, denoted as the NTE2 model. The functional forms of TE and NTE1 dose-response models used are as follows:

$$P_{\mathrm{TE}} = P_0 + [\alpha(L)D + \beta(L)D^2]e^{-\lambda(L)D} \quad (1)$$

$$P_{\mathrm{NTE}} = P_0 + [\alpha(L)D + \beta(L)D^2]e^{-\lambda(L)D} + \kappa(L)e^{-\lambda(L)D}\Theta(D_{th}) \quad (2)$$

where D is dose, P_0 is the background prevalence at an age of 600 days (irradiated 120-day-old mice and held for 16 months $= 120 + 480 = 600$ days) when animals are sacrificed and L is LET. A linear-quadratic model for the dose induction term multiplied by a cell sterilization factor was considered for the TE model, where both α and λ are LET-dependent parameters, and β (dose-squared) term is considered only for gamma rays and low-LET ions (proton and helium). The cell sterilization factor describes the concave down bending of the dose response observed at higher doses. The dose-response data for gamma rays were treated differently than the analysis used for particle beams. For the NTE1 model, we considered a LET-dependent but dose-independent constant term above a certain dose threshold represented by a step function Θ, which is arbitrarily set below the lowest dose of the experiments at 0.001 Gy. The parameter $\kappa(L)$ represents the strength of nontargeted effect. The NTE2 model is similar to Eq. (2) with the $\kappa(L)$ a constant fitted to the data independent of LET and including the step function with a threshold dose at 0.001 Gy. The dose-independent constant term above a certain dose threshold represented by a step function Θ is set below 0.001 Gy, with further considerations described below.

A smooth ''turn on'' of a bystander effect could be assumed, however, the current experiments do not address where this dose occurs and if it depends on radiation quality or the temporal patterns of irradiation. Other cell culture experiments suggest a propagation distance for bystander effects perhaps approaching 1 cm. How the strength of the signal varies with distance is not known nor if the bystander effect found in various cell culture experiments has a common mechanism with the NTE suggested by the analysis of the current experiments. Further very-low-dose experiments will be needed to study how this effect turns on at the lowest doses and to determine the mechanism that would lead to a NTE in the current mouse model.

In our earlier published studies, we had assumed the tumor prevalence to be Poisson distributed using a track structure approach to the hazard function model representing initiation promotion (*23, 24*). However, the current experiments focused on the low-dose region where the results are nearly identical to those assuming the Poisson distribution. Further work is ongoing using the track structure form of the initiation promotion hazard approach.

We consider a model where radiation quality dependence parameters increase linearly with LET with an exponentially decreasing modifying factor at high LET, as given by the equations below:

$$\alpha(L) = \alpha_0 + \alpha_1 L\exp(-\alpha_2 L) \quad (3)$$

$$\lambda(L) = \lambda_0 + \lambda_1 L\exp(-\lambda_2 L) \quad (4)$$

$$\kappa(L) = \kappa_1 L\exp(-\kappa_2 L) \quad (5)$$

where parameters α_2, λ_2 and κ_2 are saturation terms at high LET.

All statistical analysis and data fitting were done using Stata software, v. 14 (StataCorp LC, College Station, TX). Nonlinear least-

TABLE 2
Prevalence of Harderian Gland Tumors after ^{137}Cs Gamma Irradiation

		Mice		
Dose (Gy)	No. per group	No. of survivors	No. with tumors (no. of carcinomas)	Prevalence
0	390	354	17 (1)	4.97 ± 2.31
0.4	156	148	8	5.4 ± 3.7
0.8	96	90	6	6.7 ± 5.3
1.2	96	78	10	12.8 ± 7.6
1.6	96	84	17	20.2 ± 8.8

Notes. The majority of tumors found were adenoma papillomas. The number of carcinomas are indicated within the parenthesis.

squares data fitting weighted by the inverse of the variance for the prevalence was used to estimate the parameters. Goodness-of-fit tests comparing the models described were made with the Akaike information criteria (AIC), Bayesian information criteria (BIC) and adjusted R^2 tests, which take into account differences in the number of parameters in the models considered. In the AIC and BIC tests, the model with the lowest test statistic provides the optimal fit, and in the adjusted R^2 test, the model with the highest values of the test statistic provides the optimal fit to the data.

The diameter of the epithelial cell nucleus believed to be transformed into mouse HG tumors is 5.5 μm, with a cell nuclear area, A, of about 24 μm^2 (*13, 14, 25*). Using the relationship between dose, (D) and fluence (F) (in units of μm^{-2}), as $D = F \times L/6.24$ the number of ion hits per cell nucleus is given by:

$$H = \frac{6.24DA}{L} \tag{6}$$

Using the TE model, $\mathrm{RBE}_{\max}$ was calculated, and is given by the ratio of linear induction coefficients:

$$\mathrm{RBE}_{\max} = \frac{\alpha_L}{\alpha_\gamma} \tag{7}$$

An alternative approach to RBE estimates, denoted as $\mathrm{RBE}_{\gamma\mathrm{Acute}}$, compares low-dose particle responses to acute gamma-ray exposures using a linear fit for doses near 1 Gy (*14*). For the HG experiment the highest gamma-ray dose of 7 Gy is not included in the $\mathrm{RBE}_{\gamma\mathrm{Acute}}$ estimate.

For the NTE model, a dose-dependent RBE can be estimated near the crossover dose in which the linear induction term is equal to the nontargeted term. The crossover dose (D_{cr}) and dose-dependent RBE ($\mathrm{RBE}_{\mathrm{NTE}}$) is computed as follows (*22, 26*):

$$D_{cr} = \frac{\kappa(L)}{\alpha(L)} \tag{8}$$

$$\mathrm{RBE}_{\mathrm{NTE}} = \frac{\alpha(L)}{\alpha_\gamma} + \frac{\kappa(L)}{\alpha_\gamma D_L} = \mathrm{RBE}_{\max}\left(1 + \frac{D_{cr}}{D_L}\right) \tag{9}$$

For doses below D_{cr} the NTE term dominates [the last term in Eq. (2)], while for doses above D_{cr} the TE term dominates the second term in Eq. (2), and at higher doses ($D_L > D_{cr}$) the RBE limits to the TE model RBE estimate.

RESULTS

The prevalence of naturally occurring tumors in the HG is highly dependent on the genotype of the species and strain. HG tumor prevalence in female B6CF1 mice was reported as 2.6 ± 2.5% at 16 months (*14*) postirradiation. In our studies, sham-treated animals were included in each of our experimental runs to minimize intra- and interexperimental variations. HG tumors from a total of 354 control animals were collected and showed a spontaneous tumor frequency of 4.97 ± 2.31%. These results are consistent with previously reported historical data.

While tumor frequency of ^{137}Cs gamma-irradiated animals (Table 2) served as the low-LET reference for the RBE calculations in our studies, the number of tumors occurring after ^{60}Co gamma irradiation was used as the low-LET control in Alpen *et al*. (*14, 15*). Although the gamma-decay energies for ^{60}Co are 1.17 and 1.33 MeV, and that of ^{137}Cs is 0.66 MeV, comparative analysis of the tumor frequencies from the two different radiation sources revealed that the small differences in gamma-ray energies do not play a significant role in modifying HG tumor prevalence, with the one-way repeated measures test using Stata software showing no significant difference ($P = 0.57$) (Fig. 1). The blue solid line and red dashed line shown in Fig. 1A illustrate the best fit using the average of the combined raw data from the ^{137}Cs gamma-ray (new) and ^{60}Co gamma-ray (old) data. The fitted line in Fig. 1B shows the model fitting using both the old and new data. The results indicate that there is no difference between HG tumor incidence after either ^{60}Co or ^{137}Csγ rays.

To ensure that we were able to consistently replicate the historical records, we exposed animals to 600 MeV/u iron ions at NSRL using doses similar to those in the previously published studies. We estimated an LET of 175 keV/μm for the NSRL experiments, while Alpen *et al*. (*14*) reported an LET of 193 keV/μm, which corresponds to a mean kinetic energy of about 500 MeV/u at the surface of the mouse. This difference is likely due to both the NSRL setting of the 600 MeV/u beam energy at the surface of the mouse compared to the experiment by Alpen *et al*. reporting the beam extraction energy, and to the LBNL beamline having a larger amount of material compared to NSRL, leading to a slightly larger energy loss. One-way repeated ANOVA test using Stata software showed that the two iron curves (Fig. 2) were not significantly different ($P = 0.237$), and the results shown in Table 3 demonstrate that we were able to consistently replicate the historical work that was conducted at the BEVALAC at LBNL in the 1980s and 1990s.

Experimental designs and tumor frequencies for 260 MeV/u silicon and 1,000 MeV/u titanium ions are shown in Tables 4 and 5, respectively. Our results revealed that the dose-dependent HG tumor incidence data after exposure to 260 MeV/u silicon ions at 70 keV/μm lie nested between the published data of 600 MeV/u iron ions at 193 keV/μm and 670 MeV/u Neon ions at 25 keV/μm on a plot of tumor incidence versus particle dose (Fig. 3).

Animals were exposed to five dose fractions of 0.026 or 0.052 Gy of 1,000 MeV/u titanium ions delivered in five successive days (Table 5). Tumor frequencies from these animals were compared to the tumor frequencies obtained

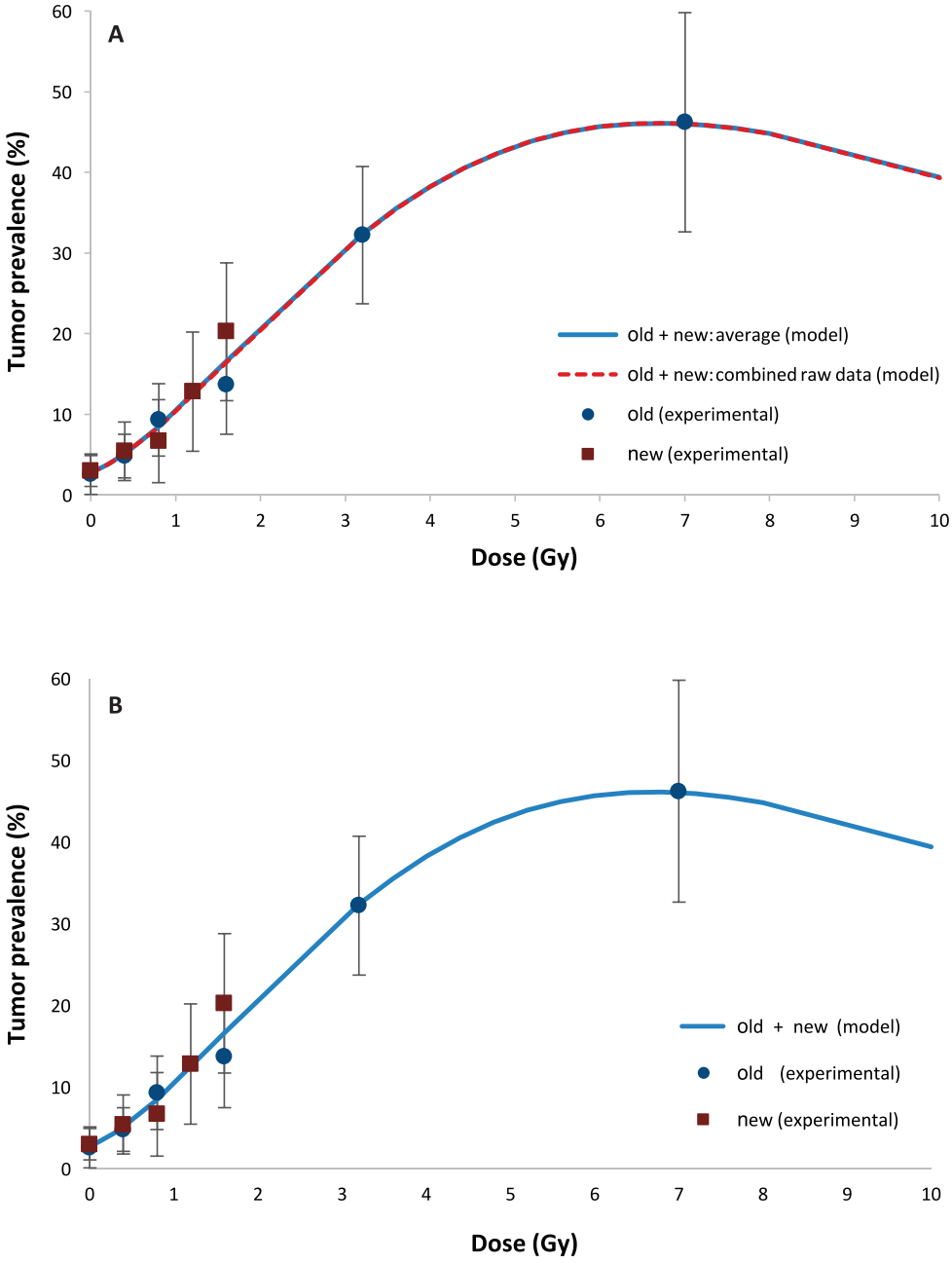

FIG. 1. Harderian gland tumor prevalence in animals 16 months after exposure to a range of gamma-ray doses. Blue circles indicate tumor prevalence after ^{60}Co gamma rays. Dark red squares indicate HG tumor prevalence after ^{137}Cs gamma rays. Error bars indicate standard deviation. Panel A: The blue solid line and red dashed line show the best fit using the average or the combined raw data from the Cs (current new) and Co gamma rays [Alpen's historical (old) data]. Panel B: The fit line shows the model fitting using the combined old and new data. The results indicate that there is no difference in HG tumor incidence after either ^{60}Co or ^{137}Cs gamma-ray irradiation.

from animals that were exposed to an acute 0.13 or 0.26 Gy dose, respectively. Based on these results, we noted that fractionating low doses of titanium over a 5-day period with 24 h intervals between fractions did not afford any sparing or additive effects on HG tumor frequency in this model system.

The similarity of the current experiments for gamma rays and iron particles with the published data from Alpen *et al.* (*14*) gave us confidence to make a global fit to both HG data sets and explore the LET and dose dependence of the tumor response. Figure 4 shows results for tumor prevalence versus absorbed dose for the silicon and titanium beams, and the global fits in the NTE1 model to these data. Although fits to each beam individually slightly improved the results, global fits are more advantageous for applications in space radiation protection. Figure 5 shows the combined data from the current experiment and the previous experiments of Alpen *et al.* (*14*) for tumor prevalence versus

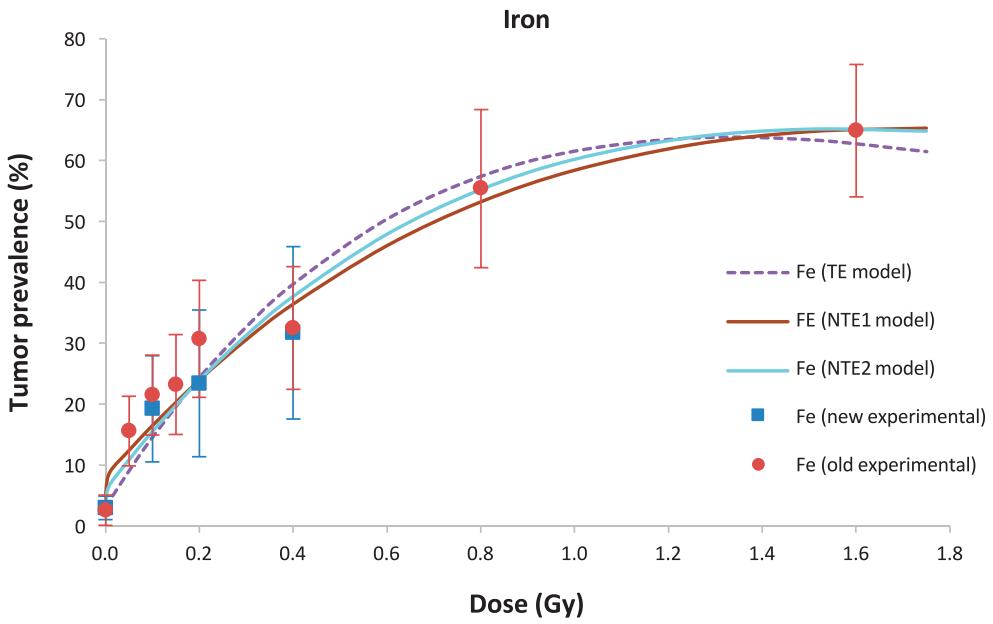

FIG. 2. Harderian gland tumor prevalence in animals exposed to a single dose of 600 MeV/u iron ions. Red circles represent data points reproduced from Alpen *et al*. (*14*). Blue square represent new data generated in our studies with the same beam at BNL. The curves show fittings using either TE, NTE or NTE2 models. Results show that there is no difference between the historical data and the tumor prevalence data generated in our project.

the number of particles per cell nucleus in comparison to the NTE1 model.

Table 6 shows values of fitted parameters in the TE, NTE1 and NTE2 described in Materials and Methods. The linear dose-response terms for the particle data were similar in each of the models considered, however, the NTE1 provided the optimal fits based on the AIC, BIC and adjusted R^2 tests, which adjust for the differences in the number of parameters in the model. The high-dose region where the β-term and cell sterilization factor play the largest role in the dose response are underrepresented in the experimental data, which resulted in the LET dependence of associated parameters (λ_1 and λ_2) not reaching statistical significance, while the overall normalization of the cell sterilization term was highly significant in each model with a P value <0.001. The NTE1 model fit better compared to the NTE2 model, however, the LET dependence of the NTE1 model response was not significant, with $\kappa_2 = 0.0028 \pm 0.0019$ ($P < 0.141$). This could indicate a role for track structure effects not adequately described by LET alone, or suggests the need for additional low-dose data.

Table 7 provides our estimates of RBEs for each particle type for the TE and NTE approaches. These results include the estimates for RBE_{max}, which considers the low-dose extrapolation, and $RBE_{\gamma Acute}$, which considers a linear fit at higher doses. Also shown are the dose-dependent RBEs in the NTE1 model with values at 0.01 Gy and 0.001 Gy shown. The gamma-ray linear slope is estimated as 4.59 ± 0.8 and 9.10 ± 0.44 Gy^{-1} for the low-dose extrapolation and high-dose regions, respectively, suggesting a dose-rate modification factor of 1.98, which is consistent with values found for other solid tumor types in various mouse strains [reviewed in ref. (*18*)]. The largest RBE values found in the TE model were 28.0 ± 6.87 and 14.1 ± 2.53 for RBE_{max} and $RBE_{\gamma Acute}$, respectively, for iron particles at 253 keV/

TABLE 3
Prevalence of Harderian Gland Tumors after 600 MeV/u Iron Irradiation

	Mice			
Dose (Gy)	No. per group	No. of survivors	No. with tumors (no. of carcinomas)	Prevalence
0	390	354	17 (1)	4.97 ± 2.31
0.1	80	78	15	19.2 ± 8.9
0.2	50	47	11	23.4 ± 12.4
0.4	50	41	13 (1)	31.7 ± 14.5

Notes. The majority of tumors found were adenoma papillomas. The number of carcinomas are indicated within the parentheses.

TABLE 4
Prevalence of Harderian Gland Tumors after 260 MeV/u Silicon Irradiation

	Mice			
Dose (Gy)	No. per group	No. of survivors	No. with tumors (no. of carcinomas)	Prevalence
0	390	354	17 (1)	4.97 ± 2.31
0.04	151	141	13	9.2 ± 4.9
0.08	132	122	16	13.1 ± 6.1
0.16	108	97	12 (1)	12.4 ± 6.7
0.32	86	74	22	29.7 ± 10.6

Notes. The majority of tumors found were adenoma papillomas. The number of carcinomas are indicated within the parentheses.

TABLE 5
Prevalence of Harderian Gland Tumors after 1,000 MeV/u Titanium Irradiation

	Mice			
Dose (Gy)	No. per group	No. of survivors	No. with tumors (no. of carcinomas)	Prevalence
0	390	354	17 (1)	4.97 ± 2.31
0.03	143	134	11	8.2 ± 4.7
0.066	125	114	10	8.8 ± 5.3
0.13	116	110	16 (1)	14.6 ± 6.7
0.26	62	55	13	23.6 ± 11.5
0.52	76	62	23 (1)	37.1 ± 12.3
5 × 0.026	120	105	15	14.3 ± 6.8
5 × 0.052	120	109	19	17.4 ± 7.3

Notes. The majority of tumors found were adenoma papillomas. The number of carcinomas are indicated within the parentheses.

μm. The RBE estimates in Table 7 are consistent with those found for other high-LET radiations, including iron particles and fission neutrons. However, the current results are unique in that the RBEs for a wide range of LETs are described, which span the types of particles found in space or used in hadron therapy. RBE estimates in the NTE1 model greatly exceed those of the $RBE_{\gamma Acute}$, reaching a value of 80 relative to acute gamma-ray exposures at 0.01 Gy for the most effective particle type. Values of RBEs in the NTE1 against the low-dose gamma-ray response estimates exceed 100 at 0.001 Gy (result not shown).

Histopathology of HG Tumors

Benign papillary adenomas are the primary type of tumors found. Histopathological evaluation of tumors found in animals exposed to ^{137}Cs gamma rays revealed that the majority of HG tumors were benign papillary adenomas. Only 1 tumor found in the group exposed to high-dose (0.4 Gy) iron ion was a malignant carcinoma. Of the 11 HG tumors found in the group exposed to 0.16 Gy silicon, only 1 tumor was found to be a carcinoma. One animal in the group exposed to 0.13 Gy titanium had a carcinoma.

DISCUSSION

The goal of our studies was to document the prevalence of tumor incidence in a sufficiently large number of animals to achieve the statistical power needed for establishing space-relevant low-dose response effects to particle radiations with LET values between 25 and 193 keV/μm. This work supplements the well-accepted HG tumorigenesis model data set in predicting LET-dependent carcinogenesis risks, and provides information to support theoretical modeling of TE and NTE at very low-particle radiation doses. Despite numerous arguments that, because the epithelial/secretory HG gland is not present in humans it may be irrelevant in predicting human risk, this animal model is nevertheless the best-studied normal epithelial tissue system that contains a uniform, nonperturbed cell population. Particle radiation-induced tumorigenesis has

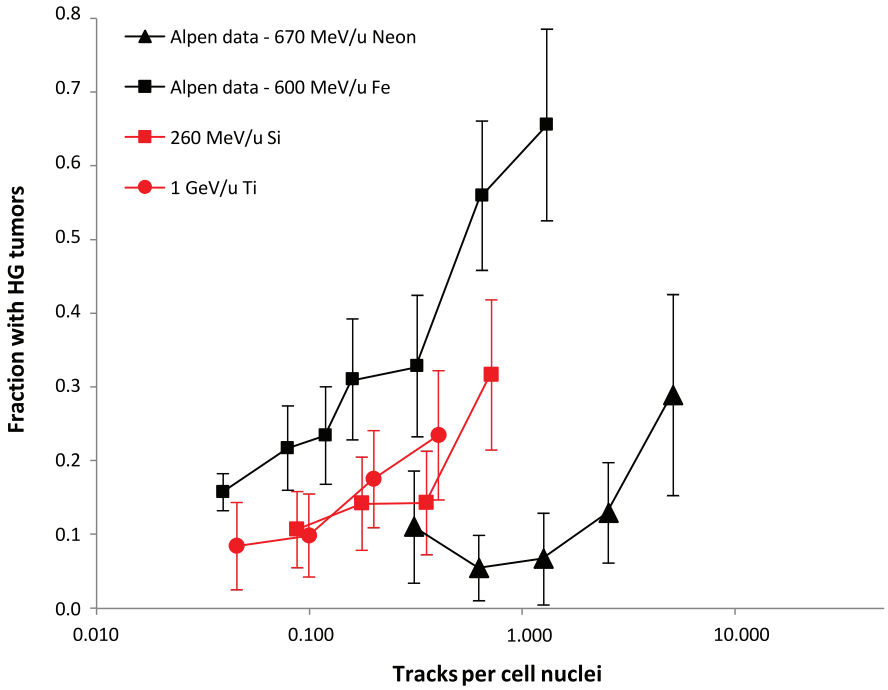

FIG. 3. Harderian gland tumor prevalence as a function of particle fluence after a single low dose of 260 MeV/u silicon (red squares; LET 70 keV/μm) or 1,000 MeV/u titanium ions (red circles; LET 100 keV/μm). Error bars indicate standard deviation. HG tumor prevalence after iron ions (LET = 193 keV/μm) and neon ions (LET = 20 keV/μm) exposure was reproduced from Alpen *et al.* (*14*) and showed that the silicon and titanium data lie nested between the two bracketing LET beams.

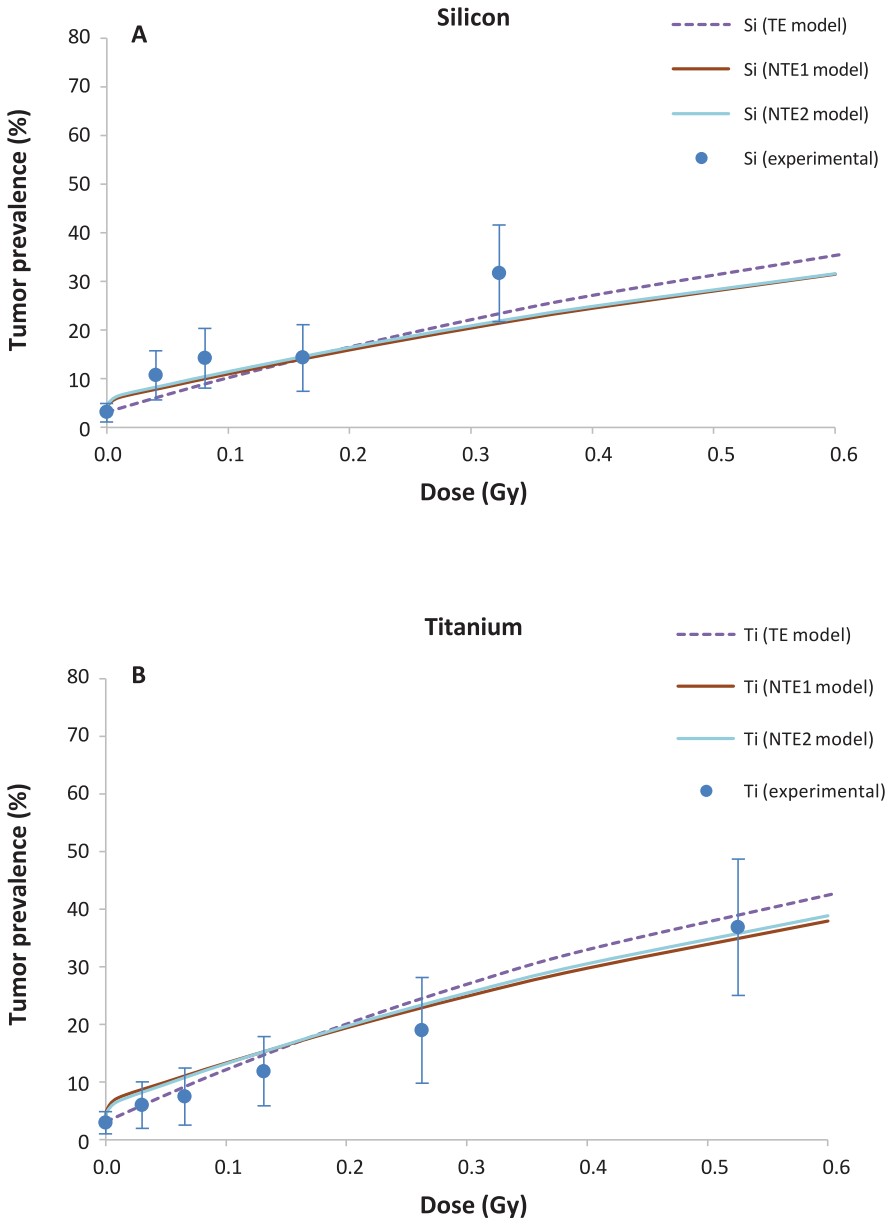

FIG. 4. TE, NTE1 and NTE2 model fitting of HG tumor prevalence in B6CF1 animals after 260 MeV/u silicon ions (panel A) and 1,000 MeV/u titanium ions (panel B). Both of the NTE models provide a better fit of the data than does the TE model.

been reported for other organ sites in animal models, such as mammary gland (*20*), skin (*27*), intestinal tract (*28*), liver and the hematopoietic system (*29*). However, the historical data reported by Fry *et al.* (*11–13*) and Alpen *et al.* (*14, 15*) on rodent HG tumorigenesis is the single most comprehensive data set of experimental observations and dose dependence available on a specific radiation-induced tumor in an experimental animal using beams of heavy ions that are found in the cosmic radiation spectrum. A limited number of reports have provided dose-response data for particle-induced tumors in other tissue sites (*11, 20, 27–32*). However, most of these tumor studies did not provide RBE estimates, due to either the lack of a dose response for the low-LET reference radiation, or other unstated reasons.

There are a number of notable differences in the methodology used for our studies and the prior published work. The earlier HG studies were conducted at the BEVALAC at LBNL using the B6CF1 animals that were originally derived from Argonne National Laboratory. The BEVALAC irradiation facility was decommissioned in the 1990s, and the B6CF1 animals had to be re-derived for our studies. The low-LET ^{60}Co gamma irradiation facility used previously at LBNL was not accessible for our studies, therefore, a ^{137}Cs gamma source was used as the reference radiation. Instead of exposing anaesthetized animals to

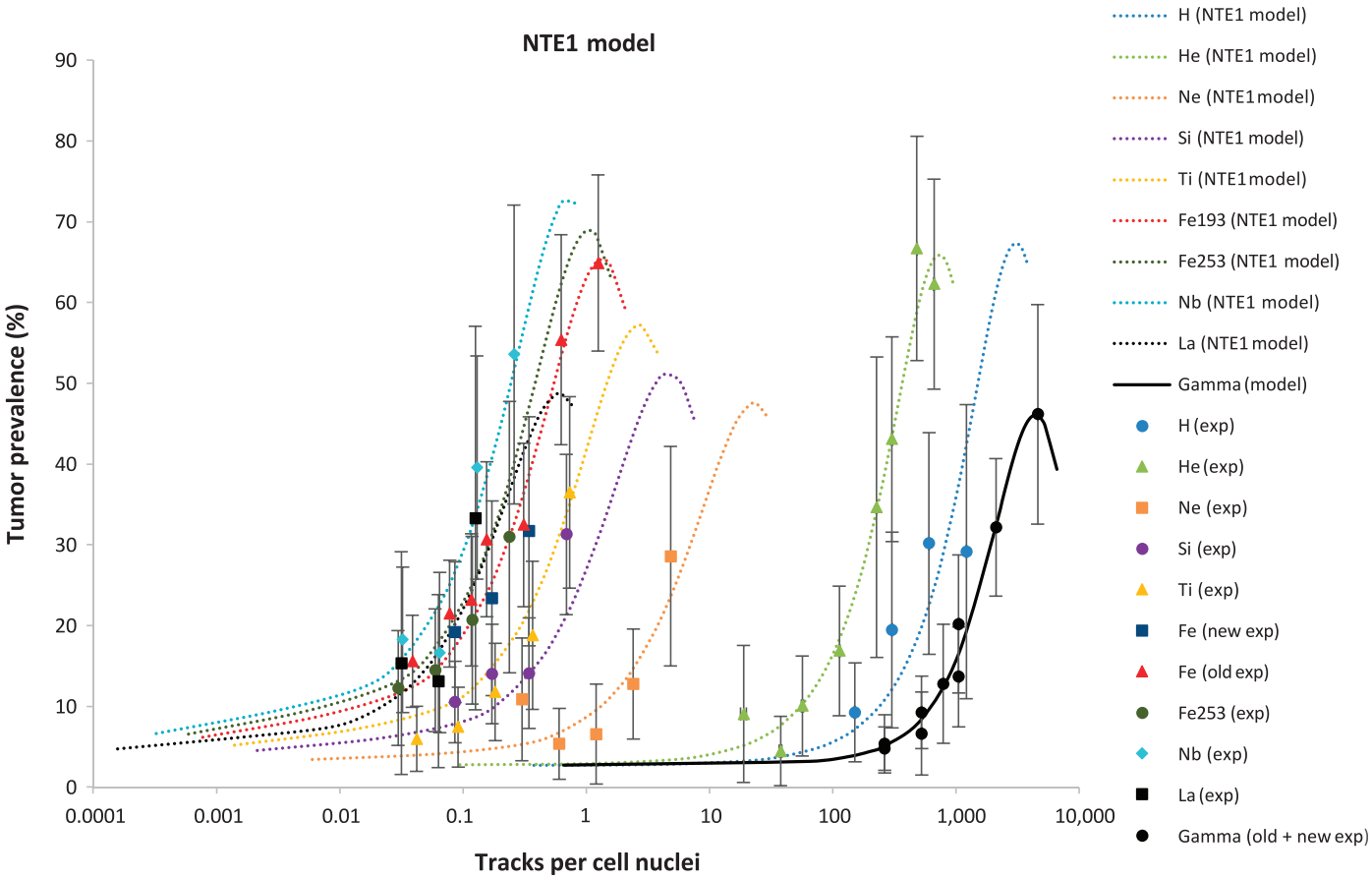

FIG. 5. Composite fittings of the percentage tumor prevalence as a function of the number of tracks per cell nuclei for all ions derived from Alpen *et al*. (*14*) studies and our study. The results clearly indicate, as reported by Alpen *et al*. (*14*), that there appears to be a saturation of target traversal that mimics saturation of tumor prevalence. The LET associated with nearly equivalent maximum effectiveness for tumor induction at 200–500 keV/μm is significantly higher than has been observed for *in vitro* transformation (*44*), cell survival or normal tissue end points (*45, 46*), which reaches a maximum at an LET of 90–150 keV/μm. Tumor induction occurs primarily at less than 1 track traversal per cell nuclei for heavy ions with LET values above 200 keV/μm.

TABLE 6
Parameter Estimates for Combined Data Sets for TE and NTE Models for the Dose Response for Percentage Tumor Prevalence

Parameter	TE	NTE1	NTE2
P_0	3.07 ± 0.36 (<10^{-4})	2.75 ± 0.34 (<10^{-4})	2.77+0.36 (<10^{-4})
α_0, Gy^{-1}	7.65 ± 3.94 (<0.058)	10.05 ± 3.56 (<0.007)	1.21 ± 4.5 (<0.789)
α_1, Gy^{-1} $(keV/\mu m)^{-1}$	1.25 ± 0.14 (<10^{-4})	0.90 ± 0.21 (<10^{-4})	1.07 ± 0.14 (<10^{-4})
α_2, $(keV/\mu m)^{-1}$	0.0038 ± 0.0004 (<10^{-4})	0.0039 ± 0.0009 (<10^{-4})	0.0036 ± 0.0003 (<10^{-4})
β, Gy^{-2}	6.02 ± 3.51 (<0.093)	4.61 ± 3.33 (<0.173)	9.24 ± 3.46 (<0.01)
λ_0, Gy^{-1}	0.243 ± 0.07 (<0.001)	0.219 ± 0.078 (<0.007)	0.286 ± 0.0533 (<10^{-4})
λ_1, Gy^{-1} $(keV/\mu m)^{-1}$	0.006 ± 0.0036 (<0.097)	0.0047 ± 0.0059 (<0.424)	0.0042 ± 0.0037 (<0.258)
λ_2, $(keV/\mu m)^{-1}$	0.0043 ± 0.0027 (<0.124)	0.0051 ± 0.0059 (<0.391)	0.0045 ± 0.0041 (<0.277)
κ_1, $(keV/\mu m)^{-1}$	-	0.048 ± 0.023 (<0.038)	3.14 ± 1.13 (<0.008)
κ_2, $(keV/\mu m)^{-1}$	-	0.0028 ± 0.0019 (<0.141)	-
Statistical tests			
Adjusted R^2	0.9248	**0.9373**	0.9337
AIC	269.6	**260.8**	263.3
BIC	285.9	**281.3**	281.7

Notes. For each statistical test considered, which adjust for the differences in the number of model parameters, the model providing the optimal fit is shown in boldface. RBE for ions using combined old and new gamma data. For the TE model, alpha = $\alpha_0 + \alpha_1 \times L \times \exp(-\alpha_2 \times L)$ and the RBE (TE) = $\alpha(L)/\alpha_\gamma$. For the NTE model, kappa = $\kappa_1 \times L \times \exp(-\kappa_2 \times L)$ with $D_{cr} = \kappa(L)/\alpha(L)$. The RBE (NTE) = RBE (TE) $(1 + D_{cr}/D_L)$.

TABLE 7
Estimates of Relative Biological Effectiveness (RBE) in Different Models and the Dose Where NTE and TE are Estimated to be Equal, D_{cr}

Z	LET (keV/μm)	RBE_{max}	$RBE_{\gamma Acute}$	D_{cr} (Gy)	RBE (NTE1) at 0.1 Gy	RBE (NTE1) at 0.01 Gy
1	0.4	1.78 ± 0.92	0.90 ± 0.44	0.0024	0.92	1.11
2	1.6	2.10 ± 0.98	1.06 ± 0.46	0.0079	1.14	1.90
10	25	7.86 ± 2.07	3.98 ± 0.81	0.031	5.19	16.3
14	70	16.3 ± 3.81	8.21 ± 1.34	0.037	11.3	38.6
22	107	21.1 ± 4.86	10.6 ± 1.69	0.039	14.8	52.5
26	175	26.2 ± 6.13	13.2 + 2.16	0.043	18.9	69.8
26	193	26.9 ± 6.36	13.6 ± 2.26	0.044	19.5	72.9
26	253	28.0 ± 6.87	14.1 ± 2.53	0.047	20.7	79.9
41	464	23.3 ± 6.89	11.8 ± 2.86	0.57	18.5	78.5
57	953	8.61 ± 3.92	4.34 ± 1.84	0.08	7.83	39.2

Notes. RBE_{max} is RBE derived from initial linear slopes at low doses of gamma rays and particle, and RBE_{Acute} is RBE derived for linear slope of low-dose particles and higher doses (~1 Gy) of acute gamma rays. RBE (NTE) is RBE in the nontargeted effects model relative to linear response at higher doses (~1 Gy) of acute gamma rays.

head-only particle beam exposures, animals in our studies were unanesthetized and whole-body irradiated. Pituitary isografts were transplanted in animals in the earlier studies with the hypothesis that elevated prolactin levels in the animals are necessary to not only initiate carcinogenesis but also to maximize the expression of induced lesions, thereby increasing the response and reducing the number of animals required to obtain significant increases in radiation-induced HG tumors above control incidences (*13*). We elected not to conduct the pituitary implant surgery in our animals, since the merits of this procedure have been under debate (*15*).[2] Since the focus of our studies was to fill the gaps in tumorigenesis data in a region of LETs that was not yet defined in the published literature, it was important for us to demonstrate that we were able to consistently replicate some of the parameters in the historical studies to anchor our studies in the comparison.

A comparative analysis of tumor data from our ^{137}Cs gamma study, and the published ^{60}Co gamma results showed that the two dose-tumor data sets are essentially identical. Tumor data for 600 MeV/u iron ions generated from exposure at NSRL overlaps with data obtained from 600 MeV/u iron ions generated from exposure at the BEVALAC, and comparison of the two data sets indicated that they were not statistically different ($P = 0.24$ using the one-way measures ANOVA test). It is also worth noting that the animals in our studies were transported by airplane from New York to California, while those in the previous studies did not require travel. Our results suggest that the added stress of transportation and perhaps other technical details did not impact HG tumor incidence. Accordingly, we have successfully demonstrated that our current approach is appropriate for these studies.

Unlike many of the animal model systems used for high-LET tumorigenesis studies, this established model system has a low and consistent spontaneous background for HG tumors, allowing us to measure tumor frequency increases at particle doses below 0.1 Gy with a reasonable number of animals in each dose group. It is this low-dose region that is most important for space radiation protection considerations. Our results showing that nontargeted effects provide an improved fit to these data, and the large deviation between TE and NTE models in this important low-dose region, suggest that possible mechanisms for NTE on tumor induction should be an important focus of future studies.

Radiation exposure of astronauts in space flight occurs at low dose and at low dose rates, and it is therefore important to evaluate the effect of dose protraction on the risk coefficient estimates. The many concepts and challenges in cancer risk prediction for the space environment have been recently reviewed (*26, 33*). Fractionation or protraction of neutrons has been reported to enhance tumorigenesis in humans and mice (*30, 32, 34*). Alpen *et al.* (*15*) completed only one HG dose protraction study of 0.07 Gy of 600 MeV/u iron ions six times with a two-week interval between exposures for a total dose of 0.42 Gy delivered in 10 weeks. Their calculated risk ratio (relative risk) of 1.47, with a 95% confidence limit of 1.30–1.68, was computed using a standard epidemiological formulation (*35*). This risk ratio is highly significant at $P < 0.01$. It was clear that the six doses, each separated by two weeks over a span of ten weeks, was about 1.5 times as effective as the same dose delivered in a single fraction.

Since it is not feasible to carry out very low-dose-rate protracted exposures at the NSRL at this time, we exposed animals to 5 dose fractions of very low doses (0.026 or 0.052 Gy) of 1,000 MeV/u titanium ions delivered in five successive days, and compared the tumor prevalence with animals that received a single acute dose of 0.13 or 0.26 Gy titanium ions. We found that there was no significant difference in tumor incidence between the two dosing regimens. The interval between irradiations has been previously reported (*15, 13*) to be important in carcinogenesis, however, those studies were generally done using higher doses (>0.2 Gy), and in some cases with dose

[2] Personal communication with RJM Fry.

fractions separated by 30 days. A fractionated regimen of 2.5 cGy/fraction of fission neutrons (fn) over a dose range of 5–40 cGy did not produce more tumors than single doses in the HG of mice (*36*), but in the case of lung adenocarcinomas in BALB/c/An NBd mice, 0.5 Gy given in two fractions separated by 30 days induced significantly more tumors than a single dose. Our results suggest that at space-relevant doses, it is likely that dose-rate effects do not occur. However, further studies using either very low-fluence strategies or doses over longer intervals between exposures may be required to completely rule out the impact of low dose rates in protracted exposures.

The NTE likely diminishes at very low doses, however, this aspect cannot be considered with the doses used in our experiments. The cell culture experiments by Nagasawa *et al.* (*25*) using alpha-particle radiation, and Yang *et al.* (*37*) using proton- and iron-particle radiation, which were performed with a much lower dose, show that a threshold exists below a dose of about 1 mGy, while the lowest dose used in the current experiment is 30 mGy. Based on these cell culture experiments, much lower doses would need to be added to our experiments to test for a threshold dose for a NTE and to elucidate how the bystander effect ''comes on'' for increasing doses. These experiments show a flat response at doses above 1 mGy, while transitioning to a linear response at higher doses.

The evidence for NTE of radiation that could potentially lead to cancer (e.g., genomic instability) is more extensive for high-LET radiation than for low-LET radiation, and is predominantly reported from *in vitro* cellular investigations (*38–40*). However, some evidence exists *in vivo* (*41*), although very few reports provide evidence at low doses of <0.1 Gy with high-LET radiations. Modeling results using the data derived from the iron, silicon and titanium studies (Figs. 3 and 4) presented here show that the NTE model gives a better fit than the TE model, providing important information on tumor incidence at space-relevant doses of heavy ions (<0.1 Gy). To our knowledge, only one published study of chromosomal aberrations in human fibroblast and lymphocyte cells has demonstrated statistically sound data at these low space-relevant dose levels of heavy ions (*42*), which were studied in our *in vivo* experiments. The data for simple exchanges, including translocations in human fibroblast cells, suggested a NTE, while the human lymphocyte results did not.

Figure 5 shows a composite NTE1 model fitting of the percentage of HG tumor prevalence after a single, individual dose exposure for each of nine particle beams (as well as for gamma rays) derived from the data reported by Alpen *et al.* (*14*) and our study, as a function of the number of tracks per cell nuclei. Several conclusions can be drawn from this plot. The NTE1 fittings indicate: 1. Tumor prevalence of much less than 15% at exposures of less than 0.05 tracks per cell nuclei; 2. An LET-dependent increase in the percentage of tumor prevalence, with the particles having higher LET values increasing beginning at 0.05 tracks per cell nuclei, whereas the lower LET radiation sources not showing increased prevalence until $>>150$ tracks per cell nuclei; 3. Very similar percentage of tumor prevalence for beams between iron and lanthanum, despite an LET range from 175 to 953 keV/μm; 4. For exposures at one track per cell nuclei, silicon ions at 70 keV/μm have a low percentage ($\sim$20%) of tumor prevalence, whereas iron ions at 193 keV/μm have $\sim$60% tumor prevalence; and 5. A predicted saturation of prevalence beyond the highest number of tracks per cell nuclei studied for each individual particle beam.

The results of the work of Cucinotta and Chappell (*22*) were iterated by introducing more detailed LET-dependent functions in a 2013 NASA report (*26*), which were identical to the functions used in the NTE1 model of the current work. Both analyses showed an improved fit with the NTE1 model compared to the TE model. However, the current results with the combined new and Alpen *et al*. experiments led to smaller values for the NTE1 model parameters κ_1 and κ_2:

Old: $\kappa_1 = 0.12 \pm 0.06$ and $\kappa_2 = 0.0053 \pm 0.002$;
New: $\kappa_1 = 0.048 \pm 0.023$ and $\kappa_2 = 0.0028 \pm 0.019$.

The RBE estimates here using the TE model are consistent with other mouse tumor induction data by high-LET radiation (*18*). Of note is that estimates based on $RBE_{\gamma Acute}$ have a smaller percentage of statistical errors compared to those of RBE_{max} estimates. The $RBE_{\gamma Acute}$ is useful for direct comparison to human epidemiology data for gamma rays, which is typically at high dose rate, and for the same dose region tested in the HG experiment (0.4–3 Gy). In addition, only a few gamma-ray experiments have been performed at sufficiently low dose rates or doses to make a confident estimate of RBE_{max}. While there is arguably a need for such experiments for estimating space radiation effects, the resources required would likely be better utilized with low-dose-rate studies using protons and other space particles (*43*). Overall, the composite space radiation-induced HG tumorigenesis data and theoretical modeling reported here represent a comprehensive documentation of evidence supporting a role for nontargeted effects for particle exposures involving one or less track per cell nucleus.

ACKNOWLEDGMENTS

The authors would like to acknowledge the support of Peter Guida, Adam Rusek, MaryAnn Petry and their staff at Brookhaven National Laboratory for their support in helping us conduct our particle radiation studies, and to Ms. Lori Chappell for support on power calculations early on in the study. The authors would also like to acknowledge the outstanding technical and animal care support by the staff at LBNL and at SRI International. This research was supported by NASA [Grant no. NNJ11HA94I (EAB)], under the auspices of the U.S. Department of Energy Office of Science (BER) under Contract No. DE-AC02-05CH11231, and by the U.S. Department of Energy [Low Dose Grant No. DE-SC0012640 (FAC)].

Received: November 23, 2015; accepted: March 3, 2016; published online: April 19, 2016

REFERENCES

1. Sigurdson AJ, Stovall M, Kleinerman RA, Maor MH, Taylor ME, Boice JD, Jr., et al. Feasibility of assessing the carcinogenicity of neutrons among neutron therapy patients. Radiat Res 2002; 157:483–9.
2. Sigurdson AJ, Ron E. Cosmic radiation exposure and cancer risk among flight crew. Cancer Invest 2004; 22:743–61.
3. Zeeb H, Blettner M, Langner I, Hammer GP, Ballard TJ, Santaquilani M, et al. Mortality from cancer and other causes among airline cabin attendants in Europe: a collaborative cohort study in eight countries. Am J Epidemiol 2003; 158:35–46.
4. Langner I, Blettner M, Gundestrup M, Storm H, Aspholm R, Auvinen A, et al. Cosmic radiation and cancer mortality among airline pilots: results from a European cohort study (ESCAPE). Radiat Environ Biophys 2004; 42:247–56.
5. Extrapolation of radiation-induced cancer risks from nonhuman experimental systems to humans. NCRP Report no. 150. Bethesda, MD: National Council on Radiation Protection and Measurements; 2005.
6. Payne AP. The harderian gland: a tercentennial review. J Anat 1994; 185 (Pt 1):1–49.
7. Coto-Montes A, Rodriguez-Colunga MJ, Tolivia D, Sanchez-Barcelo E. Histopathological features of the Harderian glands in transgenic mice carrying MMTV/N-ras protooncogene. Microsc Res Tech 1997; 38:311–4.
8. Mahler JF, Stokes W, Mann PC, Takaoka M, Maronpot RR. Spontaneous lesions in aging FVB/N mice. Toxicol Pathol 1996; 24:710–6.
9. Parnell PG, Crossland JP, Beattie RM, Dewey MJ. Frequent Harderian gland adenocarcinomas in inbred white-footed mice (Peromyscus leucopus). Comp Med 2005; 55:382–6.
10. White V, Sinn E, Albert DM. Harderian gland pathology in transgenic mice carrying the MMTV/v-Ha-ras gene. Invest Ophthalmol Vis Sci 1990; 31:577–81.
11. Fry RJM. Experimental radiation carcinogenesis: what have we learned? Radiat Res 1981; 87:224–39.
12. Fry RJM. Radiation quality and risk estimation in relation to space missions. Adv Space Res 1992; 12:403–6.
13. Fry RJM, Powers-Risius P, Alpen EL, Ainsworth EJ, Ullrich RL. High-LET radiation carcinogenesis. Adv Space Res 1983; 3:241–8.
14. Alpen EL, Powers-Risius P, Curtis SB, DeGuzman R. Tumorigenic potential of high-Z, high-LET charged-particle radiations. Radiat Res 1993; 136:382–91.
15. Alpen EL, Powers-Risius P, Curtis SB, DeGuzman R, Fry RJM. Fluence-based relative biological effectiveness for charged particle carcinogenesis in mouse Harderian gland. Adv Space Res 1994; 14:573–81.
16. Cucinotta FA. Review of NASA approach to space radiation risk assessments for Mars exploration. Health Phys 2015; 108:131–42.
17. Borek C, Hall EJ, Rossi HH. Malignant transformation in cultured hamster embryo cells produced by X-rays, 460-keV monoenergetic neutrons, and heavy ions. Cancer Res 1978; 38:2997–3005.
18. Cucinotta FA. A new approach to reduce uncertainties in space radiation cancer risk predictions. PloS One 2015; 10:e0120717.
19. Cucinotta FA, Schimmerling W, Wilson JW, Peterson LE, Saganti PB, Dicello JF. Uncertainties in estimates of the risks of late effects from space radiation. Adv Space Res 2004; 34:1383–9.
20. Dicello JF, Christian A, Cucinotta FA, Gridley DS, Kathirithamby R, Mann J, et al. In vivo mammary tumourigenesis in the Sprague-Dawley rat and microdosimetric correlates. Phys Med Biol 2004; 49:3817–30.
21. Lowenstein DI, Rusek A. Technical developments at the NASA Space Radiation Laboratory. Radiat Environ Biophys 2007; 46:91–4.
22. Cucinotta FA, Chappell LJ. Non-targeted effects and the dose response for heavy ion tumor induction. Mutat Res 2010; 687:49–53.
23. Cucinotta FA, Wilson JW. An initiation-promotion model of tumour prevalence from high-charge and energy radiations. Phys Med Biol 1994; 39:1811–31.
24. Cucinotta FA, Wilson JW. Initiation-promotion model of tumor prevalence in mice from space radiation exposures. Radiat Environ Biophys 1995; 34:145–9.
25. Nagasawa H, Peng Y, Wilson PF, Lio YC, Chen DJ, Bedford JS, et al. Role of homologous recombination in the alpha-particle-induced bystander effect for sister chromatid exchanges and chromosomal aberrations. Radiat Res 2005; 164:141–7.
26. Cucinotta FA, Kim MY, Chappell L. Space radiation cancer risk projections and uncertainties - 2012; NASA Report no. NASA/TP-2013-217375. Houston: National Aeronautics and Space Administration; 2013.
27. Burns FJ, Tang MS, Frenkel K, Nadas A, Wu F, Uddin A, et al. Induction and prevention of carcinogenesis in rat skin exposed to space radiation. Radiat Environ Biophys 2007; 46:195–9.
28. Trani D, Nelson SA, Moon BH, Swedlow JJ, Williams EM, Strawn SJ, et al. High-energy particle-induced tumorigenesis throughout the gastrointestinal tract. Radiat Res 2014; 181:162–71.
29. Weil MM, Bedford JS, Bielefeldt-Ohmann H, Ray FA, Genik PC, Ehrhart EJ, et al. Incidence of acute myeloid leukemia and hepatocellular carcinoma in mice irradiated with 1 GeV/nucleon (56)Fe ions. Radiat Res 2009; 172:213–9.
30. Spiess H, Mays CW. Exostoses induced by 224Ra (ThX) in children. Eur J Pediatr 1979; 132:271–6.
31. Spiess M, Mays CW. Radionuclide carcinogenesis. Oak Ridge, TN: USAEC Division of Technical Information Extension; 1973.
32. Ullrich RL, Jernigan MC, Cosgrove GE, Satterfield LC, Bowles ND, Storer JB. The influence of dose and dose rate on the incidence of neoplastic disease in RFM mice after neutron irradiation. Radiat Res 1976; 68:115–31.
33. Cucinotta FA, Kim MH, Chappell LJ, Huff JL. How safe is safe enough? Radiation risk for a human mission to Mars. PloS One 2013; 8:e74988.
34. Ainsworth EJ, Jordan DL, Miller M, Cooke EM, Hulesch JS. Dose rate studies with fission spectrum neutrons. Radiat Res 1976; 67:30–45.
35. Armitage P, Berry G. Statistical methods of medical research. Oxford: Blackwell Scientific Publications; 1987.
36. Fry RJM. The role of animal studies in low dose extrapolation. Washington, DC: National Council on Radiation Protection and Measurements; 1982.
37. Yang H, Magpayo N, Rusek A, Chiang IH, Sivertz M, Held KD. Effects of very low fluences of high-energy protons or iron ions on irradiated and bystander cells. Radiat Res 2011; 176:695–705.
38. Morgan WF. Non-targeted and delayed effects of exposure to ionizing radiation: I. Radiation-induced genomic instability and bystander effects in vitro. Radiat Res 2003; 159:567–80.
39. Prise KM, O'Sullivan JM. Radiation-induced bystander signalling in cancer therapy. Nat Rev Cancer 2009; 9:351–60.
40. Brenner DJ, Elliston CD. The potential impact of bystander effects on radiation risks in a Mars mission. Radiat Res 2001; 156:612–7.
41. Morgan WF. Non-targeted and delayed effects of exposure to ionizing radiation: II. Radiation-induced genomic instability and bystander effects in vivo, clastogenic factors and transgenerational effects. Radiat Res 2003; 159:581–96.
42. Hada M, Chappell LJ, Wang M, George KA, Cucinotta FA. Induction of chromosomal aberrations at fluences of less than one HZE particle per cell nucleus. Radiat Res 2014; 182:368–79.
43. Cucinotta FA, Cacao E, Alp M. Space radiation quality factors and the delta ray dose and dose-rate reduction effectiveness factor. Health Phys 2016; 110:262–6.
44. Yang TC, Craise LM, Mei MT, Tobias CA. Neoplastic cell transformation by heavy charged particles. Radiat Res 1985; 8:S177–87.
45. Alpen EL, Powers-Risius P. The relative biological effect of high-Z, high-LET charged particles for spermatogonial killing. Radiat Res 1981; 88:132–43.
46. Rodriguez A, Alpen EL, Powers-Risius P. The RBE-LET relationship for rodent intestinal crypt cell survival, testes weight loss, and multicellular spheroid cell survival after heavy-ion irradiation. Radiat Res 1992; 132:184–92.